

Development of dual-channel AOTF-based system for 3D imaging spectroscopy

Alexander Machikhin^{a,b}, Vladislav Batshev^{a,c}, Vitold Pozhar^{a,c}, Mikhail Mazur^d,
Alexander Naumov^{a*}, Alexey Gorevoy^{a,b,c}

^aLaboratory of Acousto-optic Spectroscopy, Scientific and Technological Center of Unique Instrumentation, Russian Academy of Sciences, 15 Butlerova street, Moscow, Russia 117342

^bDepartment of Electrical Engineering and Introscopy, Institute of Automatics and Computer Engineering, National Research University “Moscow Power Engineering University”, 14 Krasnokazarmennaya street, Moscow, Russia 111250

^cDepartment of Optic-electronic Devices, Bauman Moscow State Technical University, 5/1 2-ya Baumanskaya street, Moscow, Russia 105005

^dAll-Russian Scientific Research Institute of Physical-Technical and Radioengineering measurements (VNIIFTRI), Mendeleyevo, Moscow Region, Russia 141570

*Corresponding author. E-mail: naumov.aa@ntcup.ru

ABSTRACT

We consider the problem of 3D imaging spectroscopy on base of a pair of acousto-optical tunable filters (AOTFs). In such a system, quality of stereoscopic spectral images is the key factor influencing the accuracy of three-dimensional (3D) measurements and shape reconstruction. We analyze the image quality in a dual-channel AOTF-based spectrometer and proposed the optical scheme, which is free of image blur and has only aberrations of image distortion and drift. They can be eliminated by means of geometrical calibration of the imager. The optical characteristics of the system prototype are presented. The theoretical analyses and calculations of image aberrations are confirmed by experiments. The devices based on the dual-channel AOTF-based stereoscopic system may be effectively used for various 3D imaging spectroscopy applications.

Keywords: 3D imaging spectroscopy, acousto-optical tunable filter, stereoscopy, aberration analysis, optical system design.

1. INTRODUCTION

Spectral imaging enables visualization in those wavelength intervals where there is no background noise and the physical, chemical, and other properties of the analyzed objects exhibit themselves most intensively. And for various inspected substances, the tools are already developed for spectral selection of the light waves in the absorption, emission or fluorescence bands. However, there are many remote sensing, machine vision and other tasks, in which along with spectral images one requires 3D spatial information. If the object surface is not flat, 2D spectral imaging systems¹⁻⁴ do not supply enough data about the object shape and its elements location.

The straightforward approach is placing an AOTF in each channel of a stereoscopic imager⁵ (Fig. 1). If the AOTFs operating in anisotropic mode are installed in opposite manner (see below Fig. 2), this device is capable to select cross-polarized spectral images⁶. This scheme ensures detecting the object shape either with polarization glasses or with pair of monochromic digital camera.

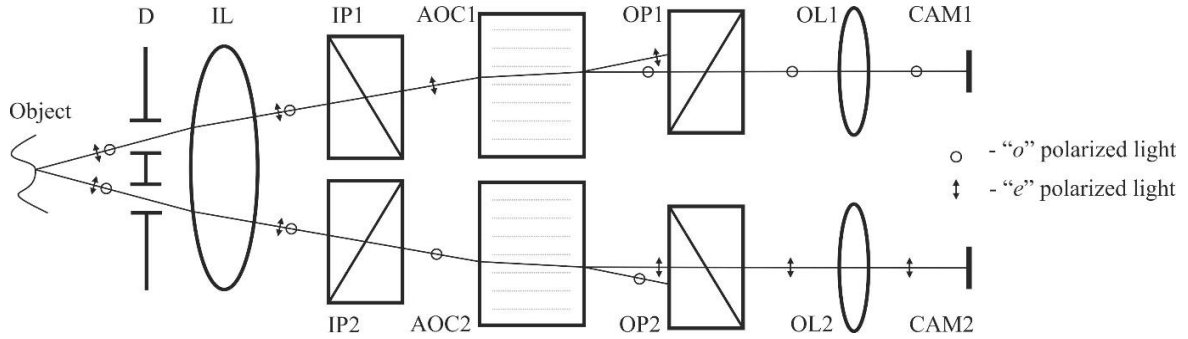


Figure 1. A concept of dual-channel AOTF-based stereovision system.

The scheme operates as follows. Diaphragm D and input lens IL form a pair of light beams, carrying the stereoscopic images of object OB, and direct them to AOTFs, each containing an acousto-optical (AO) cell AOC, input IP and output OP polarizers. The spectral component of light satisfying the Bragg condition, diffracts in each AO cell on the acoustic wave, thus changing the linear polarization direction and propagation direction. Then two orthogonally polarized monochromatic beams are focused by output lenses OL and are recorded by monochromic cameras CAM. The size of diaphragm hole forms the necessary aperture of AO cells.

The quality of stereoscopic spectral images is a key factor affecting the accuracy of 3D measurements and the shape reconstruction. AOTFs cause specific aberrations, which should be estimated at the stage of optical design⁷. In this paper, we analyze theoretically and experimentally the image aberrations in such a dual-channel AOTF-based spectrometer. We show that the proper choice of diffraction scheme and the optimization of AO cell parameters eliminate the image blur and other spot aberrations, but exhibit the image distortion and chromatic drift which still may be eliminated by means of geometrical calibration of the imager⁸⁻⁹.

2. OPTICAL SYSTEM DESIGN

We use two identical AO cells made of TeO₂ crystal with wide-aperture geometry of diffraction with cut angle $\gamma = 6^\circ$. In the first AO cell, "o"-polarized light propagates inside the crystal at angle $\theta_o = 12.2^\circ$, and after diffraction, it becomes "e"-polarized propagating at $\theta_e = 13.8^\circ$ (Fig. 2). The second AO cell has the same geometry, but it is opposed, so incident light is "e"-polarized, while diffracted light is "o"-polarized. So the scheme is also polarization sensitive.

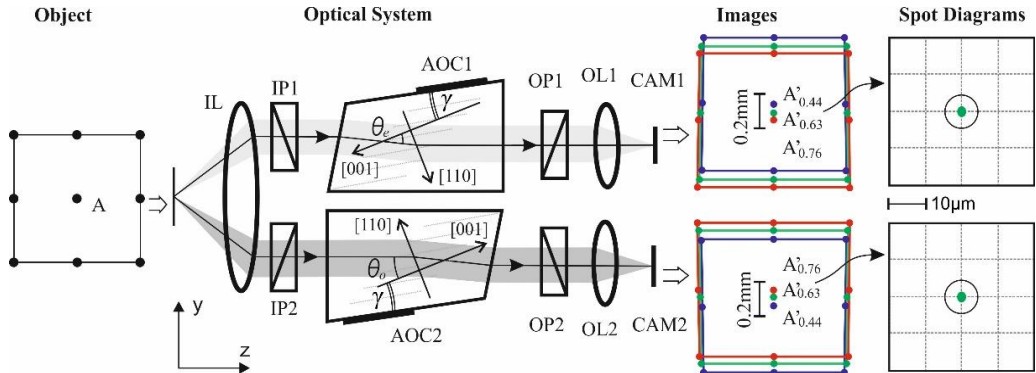


Figure 2. Aberrational analysis of the designed system.

The aberrational analysis and the optimization of the optical system were carried out in Zemax software using an original module for ray tracing through AOTF⁷. The shape of AO cells was optimized to minimize both the image distortion and the angle between the input and the output light. Since the only optimization parameter is the angle of output facet, it is not possible to satisfy two requirements. The optimized angle value is 87° , the residual angle between the input and the output light is about 2° and the distortion is less than 2%. The other AOTF parameters are the following: tuning range 440-760 nm (ultrasound frequency range 65-127 MHz), spectral resolution 2.5 nm (at $\lambda = 633$ nm), angular aperture $3^\circ \times 3^\circ$, entrance pupil 6 mm \times 8 mm.

We use photographic objective F5.6 with focal length 100 mm as an input lens IL. The focal length 50 mm of each output lens provides the field of view $5.5^\circ \times 4^\circ$, which exceeds that of the AOTF and guarantees the collection of entire light flux transmitted through AO cell. For image acquisition, we use cameras DMM 22BUC03-ML with CMOS sensors Aptina MT9V024 (744×480 , $1/3''$, pixel pitch $6 \mu\text{m} \times 6 \mu\text{m}$).

The aberrational analysis shows the almost identical image quality in both channels. We use the optical scheme with collimated beams, so that AO cells do not introduce spot aberrations, which usually restrict the image resolution⁷. Other aberrations may be determined and taken into account at geometrical calibration stage. In result, distortion is 1.8% and chromatic image drift is $181 \mu\text{m}$. The last has opposite direction in AOTFs due to their upturned orientation (Fig. 2). It should be added that the size of the scattering spot in real system is determined by the quality of lenses IL and OL.

3. EXPERIMENTS

To estimate the image quality and 3D measurement capabilities of the designed system we performed experiments with use of the test chart in form of the glass plate with chrome-etched chessboard pattern ($0.5 \text{ mm} \times 0.5 \text{ mm}$ square cell). Being illuminated by a white-light source in combination with white diffusing glass, it displays at the camera the stereoscopic spectral images like those presented in Fig. 3. Two pictures in the different channels demonstrate chromatic image drift (points 1-4). We determined the coordinates of the points⁸ and compared them to the dependence calculated in ZEMAX software. As the calculated value is 180 nm while the measured one is 168 nm we can estimate the experimental value of distortion $(a-b)/b \approx 2.1\%$ is in good correspondence with the calculated one 1.9%.

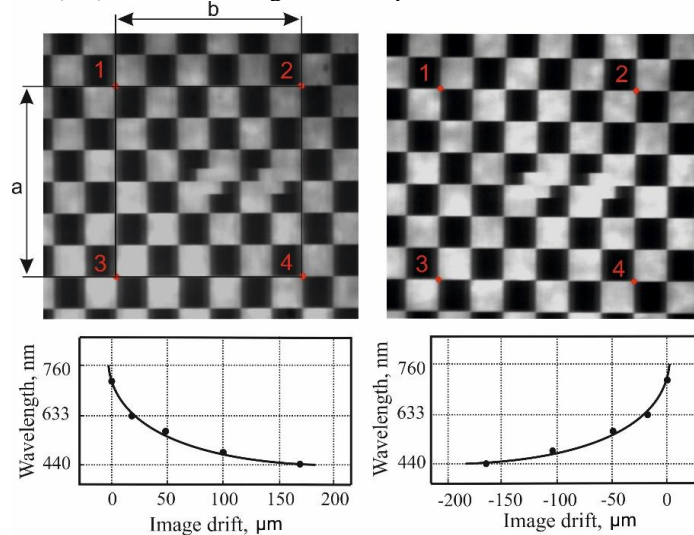


Figure 3. Stereoscopic images of the test-chart in the first and second AO cells at 633 nm.

Solid line – calculations, points – experiment.

To check the applicability of the designed system for 3D measurements, we have carried out its geometrical calibration. For this purpose, the test-chart was set approximately perpendicular to z -axis and moved it along within the distance range 194-202 mm with a given step 0.5 mm. Position of the test-chart and direction of its shift were determined during calibration, but the shift step was not known exactly. The distortion is considered to be small, so we used pure projective (pinhole) camera model. The results of the previous work¹⁰ shows that due to the small angular aperture and depth of field, this method provides greater accuracy and stability compared to the widely used alternative method⁹. It is relies on two reference values of the test chart distance, chosen usually at the near and far ends of the working range, which is called sharply depicted space.

This calibration method was applied to spectral images set collected independently at four wavelengths: 450 nm, 525 nm, 600 nm, 675 nm. The images of another series, which differs from the calibration set by 0.25 mm shift along z axis, were used for the system testing. For estimation of length measurement errors we calculated statistical values of the experimentally determined cell size in different points of the test-pattern as well as the size of 0.5 mm segment along z -axis at different distances from the image (Fig. 4).

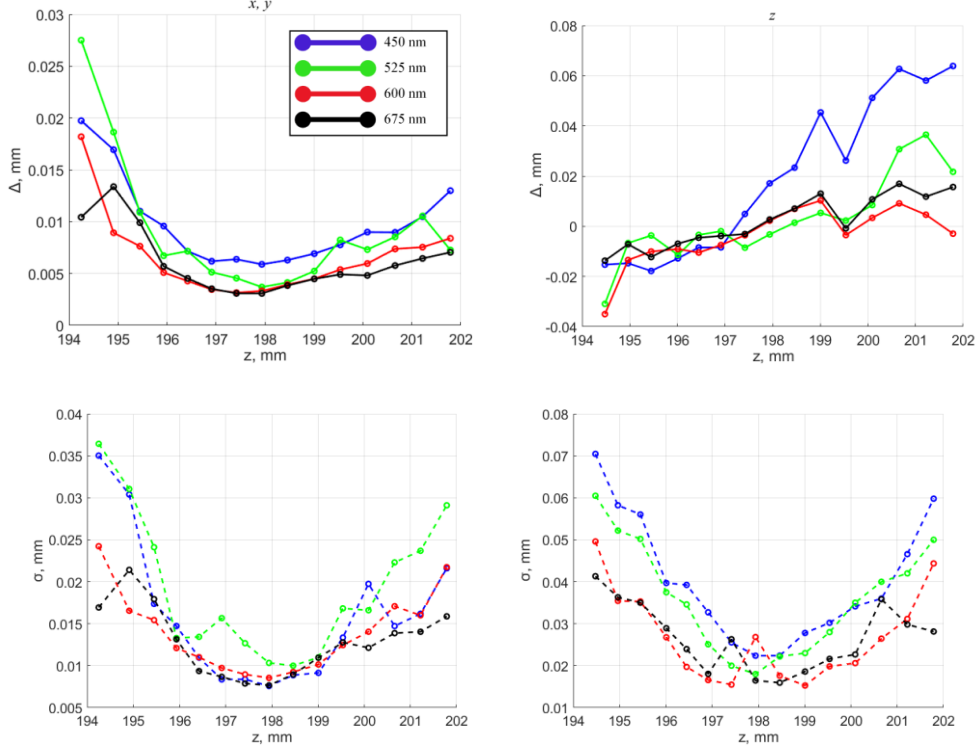


Figure 4. The statistic characteristics of testing procedure depending on the distance to the test-chart:
mean value Δ (solid) and standard deviation (σ).

These data can be considered as estimations of the systematic (Δ) and random (σ) components of the error. For convenience, we gathered the data in Table 1. The averaged values do not exceed 0.05 mm, which is acceptable for our applications. The errors are much lower in the range of 197–200 mm, where the images have maximal sharpness.

Table 1. Average values of mean value Δ and standard deviation σ in coordinates determination

Wavelength	450 nm	525 nm	575 nm	650 nm
Δ in x - y plane, mm	0.0097	0.0090	0.0065	0.0061
σ in x - y plane, mm	0.0158	0.0154	0.0138	0.0128
Δ in z direction, mm	0.0154	0.0025	-0.0134	0.0017
σ in z direction, mm	0.0401	0.0348	0.0267	0.0266

4. CONCLUSION

We have shown that image quality provided by dual-channel AOTF-based stereoscopic system is high enough for 3D measurements in arbitrary spectral subrange within the visible range. Due to collimating scheme of diffraction, the system provides high resolution and exhibits residual image distortion and spectral drift, which can be accounted by means of geometrical calibration and do not affect significantly the accuracy 3D measurements.

The results of theoretical consideration and mathematical simulation of image aberrations are confirmed by the experiments using the prototype of the AOTF-based stereoscopic imager. It is demonstrated that geometrical calibration of such imagers can be performed with use of a flat test-chart moveable along z -axis.

The stereoscopic AOTF-based imaging is promising for the development of new methods and tools for 3D imaging spectroscopy applications.

ACKNOWLEDGMENTS

Russian Science Foundation (project #19-19-00606) supported this study.

REFERENCES

- [1] M.H. Kim, T.A. Harvey, D.S. Kittle, H. Rushmeier, J. Dorsey, R.O. Prum and D.J. Brady, “3D imaging spectroscopy for measuring hyperspectral patterns on solid objects”, ACM Transactions on Graphics, 31(4), 38 (2012).
- [2] M.C. Martin, C. Dabat-Blondeau, M. Unger, J. Sedlmair, D.Y. Parkinson, H.A. Bechtel, B. Illman, J.M. Castro, M. Keilweitz, D. Buschke, B. Ogle, M.J. Nasse and C.J. Hirschmugl, “3D spectral imaging with synchrotron Fourier transform infrared spectro-micromotography”, Nature Methods, 10(9), 861-864 (2013).
- [3] <https://phenospex.com/products/plant-phenotyping/science-planete-f500-multispectral-3d-laser-scanner/>
- [4] S. Yoon and C. Thai, “Stereo spectral imaging system for plant health characterization”, Proc. ASABE Annual Int. Meeting, 096583, 1-12 (2009).
- [5] A. Machikhin and V. Pozhar, “Single-AOTF-based stereoscopic 3-dimensional spectral imaging systems based on a single acousto-optical tunable filter”, Journal of Physics: Conference Series, 661, 012041 (2015).
- [6] A. Machikhin, V. Batshev, V. Pozhar and M. Mazur, “Acousto-optical full-field stereoscopic spectrometer for 3D reconstruction in any spectral interval”, Computer Optics, 6, 871-877 (2016).
- [7] A. Machikhin, V. Batshev and V. Pozhar, “Aberration analysis of AOTF-based spectral imaging systems”, J. Opt. Soc. Am. A, 34(7), 1109-1113 (2017).
- [8] J. Mallon and P.F. Whelan, “Calibration and removal of lateral chromatic aberration in images”, Pattern Recognition Letters 28(1), 125-135 (2007).
- [9] Z. Zhang, “Flexible camera calibration by viewing a plane from unknown orientations”, Proc. Int. Conf. Comp. Vis., 666-673 (1999).